Similarity-Based Angiography (*SIMBA*) for Fast Reconstruction of Static Whole-Heart Coronary MR Images from Free-Running Acquisitions

John Heerfordt[1,2], Kevin K. Whitehead[3], Jessica A.M. Bastiaansen[1], Lorenzo Di Sopra[1], Christopher W. Roy[1], Jérôme Yerly[1,4], Mark A. Fogel[3], Matthias Stuber[1,4], and Davide Piccini[1,2]
[1]Department of Radiology, Lausanne University Hospital and University of Lausanne, Lausanne, Switzerland, [2]Advanced Clinical Imaging Technology, Siemens Healthcare, Lausanne, Switzerland, [3]Children's Hospital of Philadelphia, Philadelphia, PA, United States, [4]Center for Biomedical Imaging (CIBM), Lausanne, Switzerland

Synopsis

SIMilarity-Based Angiography (*SIMBA*) is a data-driven method for fast reconstruction of static whole-heart coronary MR angiograms from free-running acquisitions. By assessing the similarity of periodically acquired k-space readouts in the superior-inferior direction, motion-consistent angiograms can be obtained without making stringent assumptions about physiological motion. *SIMBA* demonstrated potential to reconstruct cardiac and respiratory motion-consistent images with visible coronary arteries both from non-contrast volunteer acquisitions at different field strengths and contrast-enhanced scans of pediatric patients. *SIMBA* provided improved sharpness and contrast compared to images from all the acquired data and similar vessel conspicuity as end-expiratory mid-diastolic frames of motion-resolved compressed sensing reconstructions.

Introduction

Whole-heart coronary MRA is commonly performed using ECG-triggering and respiratory gating which are often associated with complicated acquisition planning and unpredictable scan times.[1] Recently introduced free-running sequences[2–3] reduce planning complexity, guarantee fixed scan times, and offer the possibility to obtain dynamic information by retrospectively sorting the continuously collected data into different motion states.[2–6] Nevertheless, these approaches require *a priori* assumptions regarding physiological frequencies, which may vary during scans or among patients, and often exploit time-consuming motion-resolved compressed sensing reconstruction algorithms[4]. This work aims at combining operator-friendly free-running acquisitions with a novel fast image reconstruction method. We hypothesize that a subject-specific motion-consistent subset of k-space data can be identified without stringent physiological assumptions, and that standard reconstruction thereof provides a motion-suppressed static whole-heart image with conspicuous coronary arteries.

Methods

We propose a SIMilarity-Based Angiography (*SIMBA*) reconstruction technique for free-running 3D radial whole-heart coronary MRA scans. In brief, *k*-means[7] is used to cluster the MR data based on the similarity of regularly acquired superior-inferior readouts (Fig.1-*SIMBA*). Subsequently, standard gridding reconstruction of the most populated cluster produces a static 3D image.

Validation was performed using variants of a 3D free-running sequence[3] with a prototype radial Phyllotaxis trajectory[8]. N=15 free-running datasets were acquired with three different protocols: ferumoxytol[9] contrast-enhanced gradient echo (CE-GRE) under respiratory ventilation (5 pediatric patients), non-contrast fast-interrupted steady state (FISS)[6] (5 healthy volunteers), and fat-saturated bSSFP (FS-bSSFP)[3] (5 healthy volunteers). Data were acquired on 1.5T MAGNETOM Avanto^{fit} (5xCE-GRE) and Aera (3xFISS, 5xFS-bSSFP) and 3T MAGNETOM Prisma^{fit} (2xFISS) clinical scanners (Siemens Healthcare, Erlangen, Germany). Main common parameters: Resolution $(1.1\ mm)^3$, FOV $(220\ mm)^3$, 5181-5749 radial interleaves of 22-24 readouts. The fixed acquisition times were: CE-GRE 7:03min, FISS 7:53-9:33min, FS-bSSFP 14:17min. The ECG was recorded as reference.

For comparison, three whole-heart reconstructions were obtained per dataset: by gridding all collected data (*All Data*), from *SIMBA*, and by selecting an end-expiratory mid-diastolic image from a fully self-gated cardiac and respiratory motion-resolved (4 respiratory bins, 50ms cardiac resolution) compressed sensing reconstruction from a free-running framework (*FRF*)[5]. For *SIMBA*, the percentage of automatically selected data was computed, and the reconstruction time recorded. Moreover, the data's physiological origin was evaluated using ECG-timestamps and the *FRF*'s respiratory self-gating signal. For all reconstructions, sharpness was measured by fitting sigmoid functions to the blood-myocardium interface.[10] Blood-myocardium contrast ratio was quantified by comparing average signal intensities in regions of interest. Furthermore, the visibility of the coronary ostia was assessed by one author (2.5yrs.'experience). For *SIMBA* and *FRF*, the visible length and sharpness of the right coronary artery (RCA) and the combined left main (LM) + left anterior descending (LAD) coronary arteries were quantified using Soap-Bubble.[11] For statistical comparisons, two-sided paired sample t-tests, after evaluating normality (Jarque-Bera[12]), and McNemar's tests (ostia) were used with $p<0.05$ after Bonferroni correction being considered statistically significant.

Results

On average, the cluster selected by *SIMBA* contained 12.8%±1.7% of the acquired data, corresponding to 27.8%±3.7% of the radial Nyquist limit. The image reconstruction time for *SIMBA* was less than 30s on a desktop computer, while reconstructing a motion-resolved *FRF*-dataset takes several hours.

Visually, *SIMBA* removed most of the motion blurriness seen in the *All Data*-reconstructions and provided comparable quality to *FRF*, albeit with slightly increased noise (Fig.2). The selected *SIMBA*-cluster contained mainly end-expiratory data (78%±26% originated from the two most end-expiratory FRF bins). Conversely, three distinct scenarios were observed in the cardiac dimension (Fig.3).

Both *SIMBA* and *FRF* provided significantly higher blood-myocardium sharpness than *All Data*, but no significant difference was observed between the two (Fig.4a). Though blood-myocardium contrast differed between the three protocols (Fig.4b), normalized values only showed a significant improvement between *SIMBA* and *All Data* (Fig.4c). Significantly more ostia were visible with *SIMBA* and *FRF* compared to *All Data* (*All Data*: 6/30, *SIMBA*: 25/30, *FRF*: 29/30) but only non-significant differences were seen between *SIMBA* and *FRF* concerning ostia, vessel length and sharpness (Fig.5).

Discussion

SIMBA mainly selected end-expiratory data from well-defined phases of the cardiac cycle, which together with the fast-moving coronary arteries being generally visible, points towards motion-consistent data in the selected cluster. The findings that *SIMBA*-images showed better blood-myocardium sharpness and contrast than *All Data*-images and similar coronary and blood-myocardium sharpness as *FRF*-images support our hypothesis that a sharp whole-heart coronary MRA can be obtained without making *a priori* physiological assumptions. The non-significant differences between *SIMBA* and *FRF* might be explained by the fact that one *SIMBA*-image, reconstructed without compressed sensing, directly uses more data than one *FRF*-frame (~3% Nyquist), but *FRF*'s regularization means that information is shared between frames. Potentially, non-trivial ways of combining data from non-adjacent phases in the cardiac cycle can be identified with *SIMBA*, as seen when early systolic and mid-diastolic data clustered together (Fig.3). Intuitively, this result is explainable by the fact that the heart has a similar anatomical shape during those two phases. Finally, *SIMBA* may complement motion-resolved compressed sensing reconstructions by making images available quickly at the scanner console.

Conclusion

SIMBA provides a means of automatically selecting motion-consistent data from free-running acquisitions of the heart without making *a priori* physiological assumptions, allowing for fast reconstruction of whole-heart coronary MRA with comparable quality to that obtained with a much longer iterative reconstruction.

Acknowledgements

No acknowledgement found.

References

1. Dweck MR, Puntman V, Vesey AT, Fayad ZA, Nagel E. MR Imaging of Coronary Arteries and Plaques. JACC Cardiovasc. Imaging 2016;9:306–316 doi: 10.1016/j.jcmg.2015.12.003.

2. Pang J, Sharif B, Fan Z, et al. ECG and navigator-free four-dimensional whole-heart coronary MRA for simultaneous visualization of cardiac anatomy and function. Magn. Reson. Med. 2014;72:1208–1217 doi: 10.1002/mrm.25450.

3. Coppo S, Piccini D, Bonanno G, et al. Free-running 4D whole-heart self-navigated golden angle MRI: Initial results. Magn. Reson. Med. 2015;74:1306–1316 doi: 10.1002/mrm.25523.

4. Feng L, Coppo S, Piccini D, et al. 5D whole-heart sparse MRI. Magn. Reson. Med. 2018;79:826–838 doi: 10.1002/mrm.26745.

5. Di Sopra L, Piccini D, Coppo S, Stuber M, Yerly J. An automated approach to fully self-gated free-running cardiac and respiratory motion-resolved 5D whole-heart MRI. Magn. Reson. Med. 2019;82:2118–2132 doi: 10.1002/mrm.27898.

6. Bastiaansen JAM, Piccini D, Di Sopra L, et al. Natively fat-suppressed 5D whole-heart MRI with a radial free-running fast-interrupted steady-state (FISS) sequence at 1.5T and 3T. Magn. Reson. Med. 2020;83:45–55 doi: 10.1002/mrm.27942.

7. MacQueen J. Some methods for classification and analysis of multivariate observations. In: Proceedings of the Fifth Berkeley Symposium on Mathematical Statistics and Probability, Volume 1: Statistics. Fifth Berkeley Symposium on Mathematical Statistics and Probability. Berkeley, Calif.: University of California Press; 1967. pp. 281–297.

8. Piccini D, Littmann A, Nielles-Vallespin S, Zenge MO. Spiral phyllotaxis: The natural way to construct a 3D radial trajectory in MRI. Magn. Reson. Med. 2011;66:1049–1056 doi: 10.1002/mrm.22898.

9. Prince MR, Zhang HL, Chabra SG, Jacobs P, Wang Y. A pilot investigation of new superparamagnetic iron oxide (ferumoxytol) as a contrast agent for cardiovascular MRI. J. Xray. Sci. Technol. 2003;11:231–40.

10. Ahmad R, Ding Y, Simonetti OP. Edge Sharpness Assessment by Parametric Modeling: Application to Magnetic Resonance Imaging. Concepts Magn. Reson. Part A. Bridg. Educ. Res. 2015;44:138–149 doi: 10.1002/cmr.a.21339.

11. Etienne A, Botnar RM, Van Muiswinkel AMC, Boesiger P, Manning WJ, Stuber M. "Soap-Bubble" visualization and quantitative analysis of 3D coronary magnetic resonance angiograms. Magn. Reson. Med. 2002;48:658–666 doi: 10.1002/mrm.10253.

12. Jarque CM, Bera AK. A Test for Normality of Observations and Regression Residuals. Int. Stat. Rev. / Rev. Int. Stat. 1987;55:163–172 doi: 10.2307/1403192.

Figures

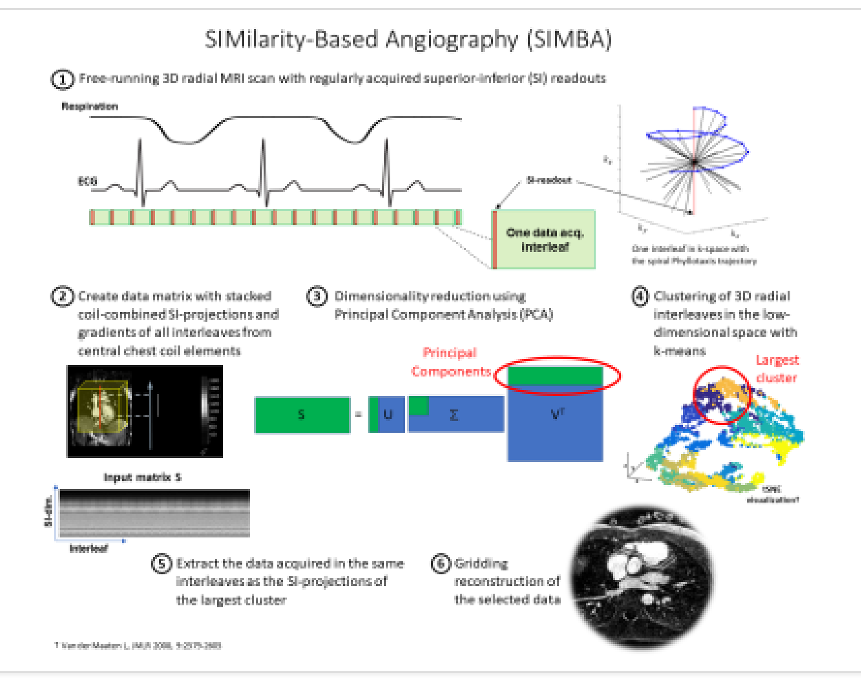

Figure 1. *SIMBA* aims at reconstructing a motion-consistent sharp image from a subset of the data from a free-running scan with periodically acquired SI-readouts. To facilitate the similarity-based clustering, the dimensionality is first reduced with PCA. Empirically it was found that extracting N=20-100 principal components provided satisfactory results (N=42 was used in this work). The *k*-means clustering is performed in the N-dimensional space created from the principal components. *k* was chosen between 11-13 to minimize the most populated cluster's intra-cluster-distance.

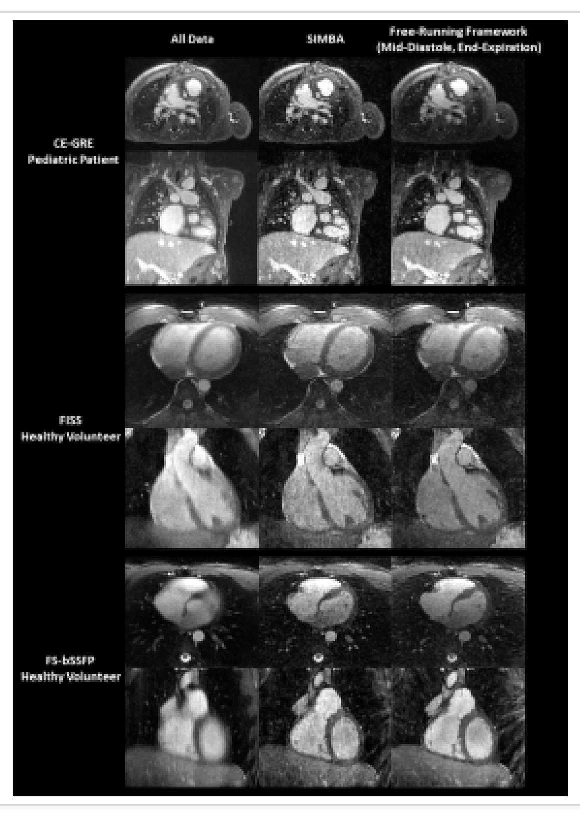

Figure 2. Example images from three different subjects scanned with free-running 3D radial acquisitions of different kinds and reconstructed with: *All Data* - left column, *SIMBA* - middle column and *FRF* - right column. In general, the *SIMBA*-images appear sharper than their *All Data* counterparts. The fact that the *FRF*-images show more homogeneous signal than those from *SIMBA* may be attributed to a combination of more motion-consistent data and the use of total-variation regularization.

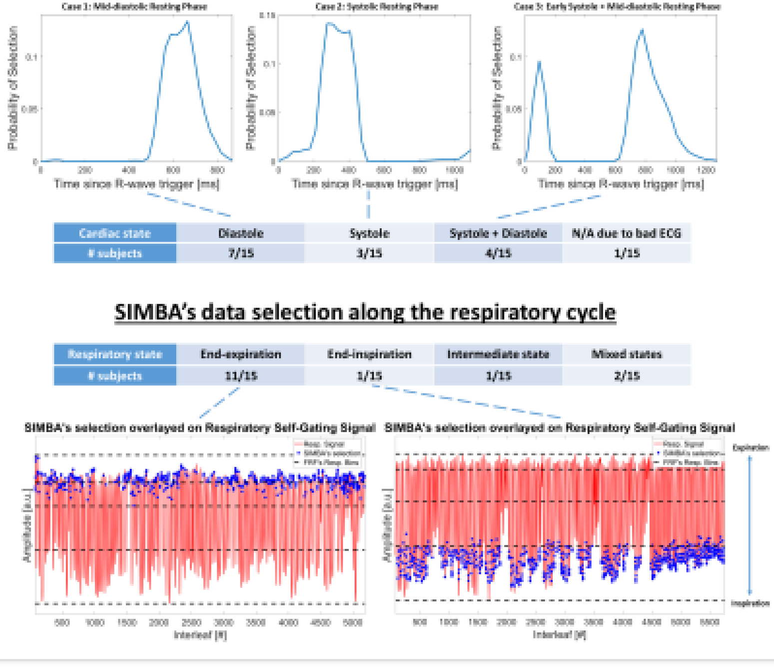

Figure 3. Three main cardiac data selection scenarios occurred with *SIMBA*: mid-diastolic data, late systolic data or a combination of early systolic and mid-diastolic data. The latter is interesting since the heart is likely to have a similar shape during those two points of the cardiac cycle, but it does not correspond to how one would conventionally extract data from an ECG. Moreover, *SIMBA* mainly selected data from the most common respiratory state, end-expiration. In two subjects *SIMBA* failed to separate different respiratory states from one another, which degraded image quality.

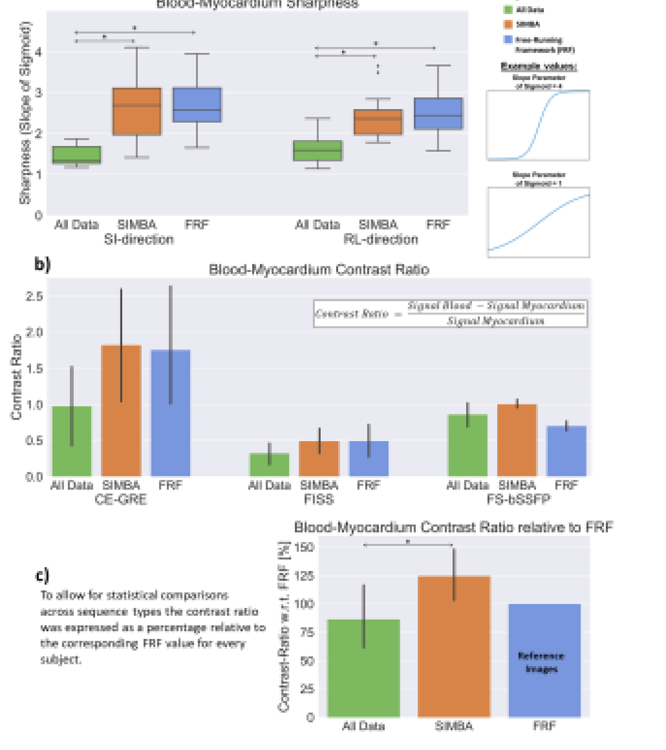

Figure 4.

a) The blood-myocardium sharpness in the superior-inferior (SI) and right-left (RL) directions obtained from fitting sigmoid functions to the interface and using the average of three slope parameter values per direction as a sharpness measure.

b) Barplots showing the average blood-myocardium contrast ratio with confidence intervals. As expected, CE-GRE provided best contrast.

c) To allow for statistical comparisons with N=15, normalization was performed by expressing the individual subjects' contrast ratio values as a percentage of the corresponding *FRF* values.

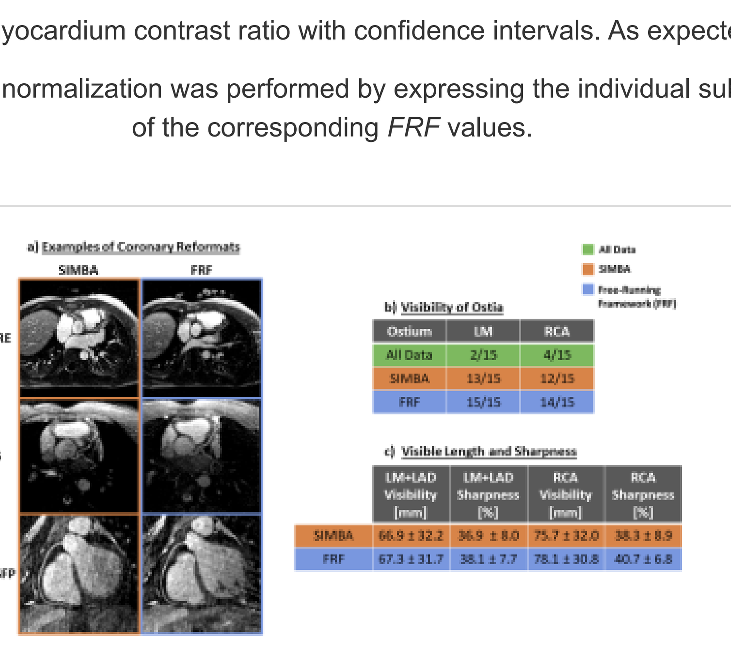

Figure 5.

a) Examples of coronary reformats from *SIMBA* and *FRF*. From this CE-GRE scan of a pediatric patient with an anomalous RCA, *SIMBA* extracted a systolic image which explains the anatomical difference compared to the mid-diastolic *FRF* image.

b) In images from *All Data*, only a handful ostia were considered visible whereas in the *SIMBA* and *FRF* images the majority were seen.

c) No significant differences in visible vessel length and sharpness of the LM + LAD and RCA were found in the vessels were both *SIMBA* and *FRF* could visualize the ostia, although *FRF* provided slightly higher values.